

# Role of package headspace on multilayer films subjected to high hydrostatic pressure

Saleh Al-Ghamdi<sup>1,2</sup>  | Barbara Rasco<sup>3</sup> | Juming Tang<sup>1</sup> | Gustavo V. Barbosa-Cánovas<sup>1</sup> | Shyam S. Sablani<sup>1</sup> 

<sup>1</sup>Biological Systems Engineering Department, Washington State University, Pullman, WA

<sup>2</sup>Department of Agricultural Engineering, College of Food and Agricultural Sciences, King Saud University, Riyadh, Saudi Arabia

<sup>3</sup>School of Food Science, Washington State University, Pullman, WA

## Correspondence

Shyam S. Sablani, Biological Systems Engineering Department, Washington State University, Pullman, WA 99164-6120.  
Email: ssablani@wsu.edu

## Funding information

National Institute of Food and Agriculture, Grant/Award Number: 2016-67017-24597; Washington State University Agriculture Experiment Station; USDA NIFA, Grant/Award Number: 2016-67017-24597

The objective of this study was to systematically examine the effect of high-pressure processing and package headspace on package integrity and properties. Working pressures were 400 and 600 MPa, and starting vessel temperatures were 30°C, 60°C, and 90°C. Coextruded and laminated multilayers packaging films were studied: film A: (PA/EVOH/PP) and film B: (PET-AlO<sub>x</sub>-OC/PA6/PP), respectively. The films were made into pouches (0.05 m × 0.10 m) and filled with 30-mL water as a model food. Various headspace volumes (0, 0.05, 0.10, 0.15, 0.20, 0.25, and 0.30-cc air/mL H<sub>2</sub>O) were introduced into the packaging before processing. Imaging was used to quantify defects such as the formation of white spots on the package surface and delamination of film layers. The results showed that the headspace level and processing initial temperature had a greater effect than the operating pressure on visual defects. The package with 0% headspace did not show any physical damage to the tested films. Furthermore, thermal and mechanical analyses showed that the coextruded film A had better resistance to testing conditions than the laminated structure of film B. The X-ray diffraction results showed that film B had more defects than film A that altered the crystalline structure. Visual observation revealed white spots and delamination in the inside layer (PP) in both films. The same processing conditions affected the oxygen and water vapour transmission rates of film B more than film A. This work provides a basic guideline to select the right headspace for a given type of packaged food whenever heat and pressure are used simultaneously.

## KEYWORDS

delamination, gas-barrier properties, mechanical properties, thermal properties, white spots, whitening stress

## 1 | INTRODUCTION

The first part of a packaged food product that a consumer sees is the packaging. If the package is even slightly damaged, consumers are less likely to purchase the product. To ensure food safety and quality, manufacturers do not release food products with damaged packaging to the market. Therefore, packaging must be able to withstand food processing operations and handling conditions and pass a rigorous inspection on package integrity before being released to the market. In high-

pressure processing (HPP), packaging must be able to transmit pressure, resist water penetration, and survive process temperatures. Plastic packaging is compatible with high-pressure and high-temperature processes.

The HPP is gaining market share in Europe and the United States as an alternative method to traditional thermal processing.<sup>1,2</sup> High pressure can improve the functional properties of foods by enhancing gel formation and inactivating certain enzymes. The popularity of HPP can be attributed to the high quality of food products that are produced

with this technology. For example, HPP can inactivate the browning enzyme polyphenoloxidase, extending the shelf life of guacamole.<sup>3-5</sup>

The high-pressure-assisted thermal sterilization (PATS) of mashed potatoes was accepted by the US Food and Drug Administration (FDA) in 2009.<sup>1</sup> However, one of the main challenges of PATS processing is the nonreversible physical damage to the packaging material,<sup>6</sup> including delamination or white spots<sup>7</sup> and/or changes in the structural and barrier properties of multilayer films.<sup>8</sup> This problem with monolayer and multilayer films was first identified as high-pressure research grew in the late 1990s. Delamination between multilayers and the loss of transparency in monolayer films was first documented by Fradin et al, in 1998.<sup>7</sup> Although this problem is yet to be fully understood and solved,<sup>9-13</sup> an early suggestion was to reduce headspace and use a vacuum. Fradin and others<sup>7</sup> studied slow decompression in HPP to reduce the damage for food packaging materials, but they did not obtain better results.

The delamination of multilayer polymeric packaging films under high-pressure and high-temperature processing has led to much speculation about HPP and package compatibility. The degree of physical damage may depend upon the level of pressure and temperature. Arguments have been made that these types of packages may not be durable enough for HPP for various reasons.<sup>14</sup> Therefore, redesigned packaging films may be needed for these applications. Recent innovations on equipment design aim to reduce damage to the packaging materials (patent numbers EP2308325 and US2011007341).<sup>1,15</sup> However, slow decompression would require the incorporation of slow-pressure release valves into the HPP units, increasing the cost of HPP equipment significantly.

Several studies have investigated the influence of high-pressure and high-temperature processing on packaging defects.<sup>10,16</sup> Most studies have focused on pressures ranging from 50 to 800 MPa and temperatures between 25°C and 95°C. These studies examined coextruded and laminated film structures,<sup>17,18</sup> including vacuum packaging with a minimal or fixed level of headspace. Fradin et al<sup>7</sup> recommended further research to investigate the effect of the package headspace on its performance and integrity. The research on the packaging headspace subjected to high-pressure and high-temperature processes is limited.

In this study, we investigated the influence of headspace, pressure, and temperature on the performance of polymeric packaging. We evaluated the performance of newly developed coextruded and laminated polymeric film structures by determining the characteristics of physical defects and the thermal, mechanical, gas barrier, and structural properties.

## 2 | MATERIALS AND METHODS

### 2.1 | High-pressure processing

High-pressure and high-temperature processing was performed in a 2-L capacity high-pressure machine (Engineered Pressure Systems, Inc. Haverhill, MA). The high-pressure pump was supplied by Hochdruck-Systeme (AM Mühlfeld 9 A-7032, Sigless, Austria) and set at 400 and 600 MPa. Starting vessel temperatures were set at 30°C, 60°C,

and 90°C. The pressurizing medium was a 10% aqueous Hydrolubric 123-B solution. A polyoxymethylene-based cylindrical sleeve (1-cm thick × 8-cm inner diameter × 22-cm depth) was used for insulation to minimize heat loss from the heating/pressurizing medium to the vessel. The vessel's inner dimensions were 10-cm diameter × 24-cm depth. The total processing time was 6 minutes (360 seconds), with a come-up time of 30 seconds, a decompression time of 30 seconds, and a holding time of 300 seconds. The temperature inside the high-pressure vessel was monitored using three thermocouple probes (K-type; Omega Engineering, Inc., Stamford, CT).

### 2.2 | Package preparation

Two types of multilayer films were used to create pouches (0.05 m × 0.10 m). Film A was an EVOH-based coextruded film consisting of three layers of oriented polyamide, 27% mol ethylene vinyl alcohol, and casted polypropylene (PA 15 µm/EVOH 15 µm/CPP 60 µm). These film layers in brackets arranged from the outside towards environment to the inside layer (sealant) towards model food. Film B was a polyethylene terephthalate coated with an organic coating and aluminum oxide laminated with polyamide 6 and polypropylene (PET 12 µm -AlO<sub>x</sub>- OC 5-6 µm/PA 6 15 µm/CPP 50 µm), respectively. Coextruded and coated-PET based laminated structures were chosen to represent the types of packaging commonly used for the commercial pasteurization and sterilization processes. After performing preliminary studies using extreme conditions of pressure and temperature (600 MPa and 90°C), these two structures were selected among four EVOH-based coextruded and six coated PET structures. The EVOH-based structures contained different grades of EVOH and protective layers. The coated structures contained AlO<sub>x</sub>-based and SiO<sub>x</sub>-based coatings, with layers protecting these coatings. The multilayer structures were supplied by collaborating polymer processing companies. Initially, an impulse sealer (MP-12; J.J. Elemer Corp. St. Louis, MO) was used to seal three sides of the pouches. The seal width was 1.5 ± 0.5 mm, and sealing was performed at 150°C for 3 seconds. The pouches were filled with 30 mL of distilled water as a food simulant and then sealed using a vacuum sealer (Easy-Pack UltraSource. LLC. Kansas, MO) that was operated for 5 seconds on the high-vacuum setting, with a pump flow capacity of 16 m<sup>3</sup>/h and a sealing temperature of 160°C.

The pouches were preheated in a water bath that was maintained at set temperatures of 30°C, 60°C, or 90°C prior to the pressure treatments. A rubber septum self-adhesive was placed on the pouch. A predetermined volume of air was injected through the septum with an airtight syringe to obtain headspaces of 0, 0.05, 0.10, 0.15, 0.20, 0.25, and 0.30-cc air/mL H<sub>2</sub>O.

### 2.3 | Films characterization

#### 2.3.1 | Defect measurement

A high-resolution scanner (Canon MG2900 Series, Ota, Japan) was used to obtain images of the processed pouches. These images

showed white spots as defects. To calculate the area of white spots, the images were transferred to an RGB (red, green, and blue) scale using an image processor (ImageJ 1.5, National Institute of Health, Bethesda, MD). The white spots, as illustrated in Figure 1, were replaced by the red colour, and the total number of pixels of the defects on the package was calculated. The area was measured by selecting the transferred total number of pixels, red pixels, with the yellow boundary line, as shown. The average image resolution was  $1800 \times 1300$  pixels, with a ratio of  $1 \text{ mm}/12 \text{ pixels} = 144 \text{ pixels per } 1 \text{ mm}^2$ . The total number of pixels was then converted to the total area by correlating known objects, such as the gridded background shown in the image. The area of the white spot defect was expressed as a percentage of the entire package area of  $5 \times 10^{-3} \text{ m}^2$ .

### 2.3.2 | Colour and thickness

White spot and transparent film colour values ( $L^*$ ,  $a^*$ ,  $b^*$ ) were measured using a colorimeter (Minolta CR 200, Konica Sensing America Inc., Ramsey, NJ). Lightness ( $L^*$ ) values of the white spots and the pouch were also compared with a white standard printing paper (lightness value was 92), illustrating the severity of the process on the transparent packages.<sup>19</sup> The film thickness of unprocessed and processed pouches and at white spot defects were measured using an electronic disc micrometer (model 15769, Flexbar Machine Co. Islandia, NY). At least, three replicate readings were taken during each measurement at various locations on the packaging.

### 2.3.3 | Thermal analysis

A differential scanning calorimeter (DSC, model Q2000 TA instrument, New Castle, DE) was utilized to determine the melting temperature and enthalpy of unprocessed and processed films and the white spots of the film. Film samples weighing 5 to 10 mg were hermetically sealed in small pans and placed in the DSC instrument along with an empty reference pan. The sample was then heated from  $25^\circ\text{C}$  to  $300^\circ\text{C}$  at a rate of  $10^\circ\text{C}/\text{min}$ . DSC thermograms were analyzed to determine the melting temperatures ( $T_m$ ) and enthalpy ( $\Delta H$ ) of each layer in the multilayer.<sup>8</sup>

### 2.3.4 | Mechanical properties

The pouches subjected to 600 MPa and  $90^\circ\text{C}$  with 0.30-cc air/mL  $\text{H}_2\text{O}$  headspace were analysed for mechanical properties measurements. Both processed and unprocessed pouches were cut into  $10 \times 2.5$ -cm sections, prepared, and conditioned for 48 hours at  $23^\circ\text{C} \pm 2^\circ\text{C}$  and  $50\% \pm 10\% \text{ RH}$  prior to mechanical testing. The film samples cut from processed pouches did not include white spots for tensile testing. For the tensile test, tensile grips attached to mechanical property analyser TA-XT2 (Stable Micro Systems Ltd. Surrey GU7 1YL, United Kingdom) were used with an initial crosshead speed (grips separation) of 50 mm/min. Both the tensile and the sealing strengths were determined according to ASTM D882-12 and F88/F88 M-15 standards, respectively. The sealing strength was determined after cutting and conditioning the samples of  $10 \times 2.5$  cm, following technique A in F88/F88 M-15. The film samples tested for sealing strength included the white spots on the film edges. The sealing section ( $1.5 \pm 0.5$  mm) was in the middle of the cut, perpendicular to the mechanical force applied, and unsupported free in the air between the grips.

### 2.3.5 | Barrier properties

Oxygen transmission rates (OTRs) were measured using a Mocon oxygen permeation analyser (Ox-Tran 2/21 MH, Modern Control, Minneapolis, MN) at  $23^\circ\text{C}$ , 55% RH, and 1 atm. Testing was performed according to ASTM D3985 standard. Water vapour transmission rates (WVTRs) were measured using a Mocon Permatran 3/33 instrument (Modern Control, Minneapolis, MN). An infrared detector was used to detect the WVTR at 100% RH and  $37.8^\circ\text{C}$ . The WVTR of the film was conducted as per ASTM F 372-99. Specimens were prepared by cutting the films to an appropriate size of  $50 \text{ cm}^2$  and mounting them inside the chambers.<sup>8</sup>

### 2.3.6 | X-ray diffraction

X-ray diffraction profiles of untreated and treated films and white spots were obtained using a diffractometer (Model Miniflex 600,

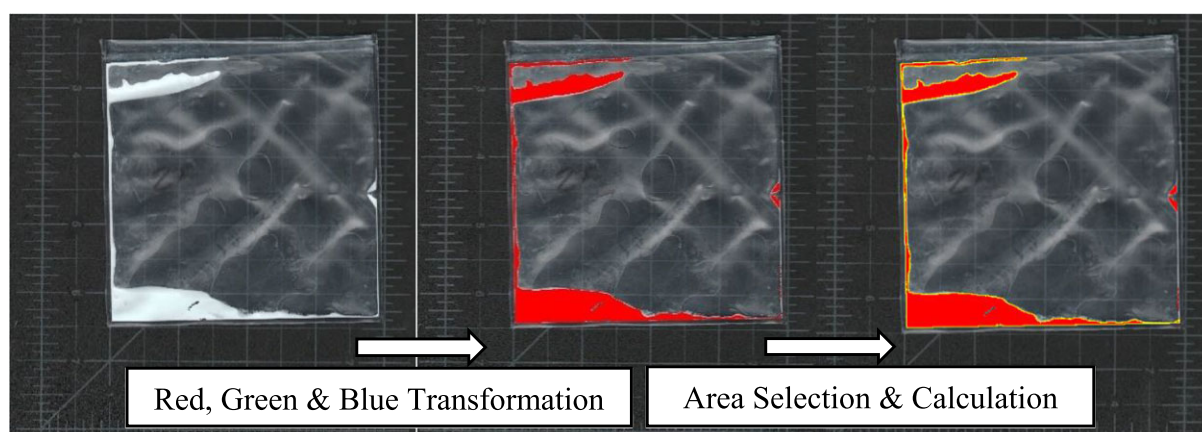


**FIGURE 1** Image transformation and area selection of film a processed at 600 MPa and  $90^\circ\text{C}$

Rigaku Americas, Woodland, TX). Each layer of multilayer structure was identified using the International Centre for Diffraction Data (ICDD) database (Newtown Square, PA) and confirmed with the literature. Experimental conditions were 40 kV, 15 mA, slit angle of  $0.02^\circ$  and a scanning speed of  $1^\circ/\text{min}$  ranging from 8 to  $35^\circ$ . The radiation of  $K\alpha$  was at  $\lambda = 1.5418 \text{ \AA}$ . The X-ray peaks were analysed for crystallinity percentage using crystallinity % =  $[I_{\text{crystal}}/(I_{\text{crystal}} + I_{\text{amorphous}})] \times 100$ , where  $I$  is the integrated area under the curve.<sup>20</sup>

## 2.4 | Statistical analysis

The data were analyzed using OriginPro 8 (OriginLab Inc., MA) and SAS 9.4 (SAS Institute Inc., Cary, NC). Tukey's honestly significant difference (HSD) test was conducted to determine the significant difference between the means at a 95% confidence interval  $\alpha = 0.05$ . All experiments were conducted in triplicate unless otherwise noted.

## 3 | RESULTS AND DISCUSSION

The high-pressure and high-temperature processes profiles are provided first and followed by the characterization of the defect of the films and a discussion of the physical, thermal, mechanical, barrier, and structural properties of the films.

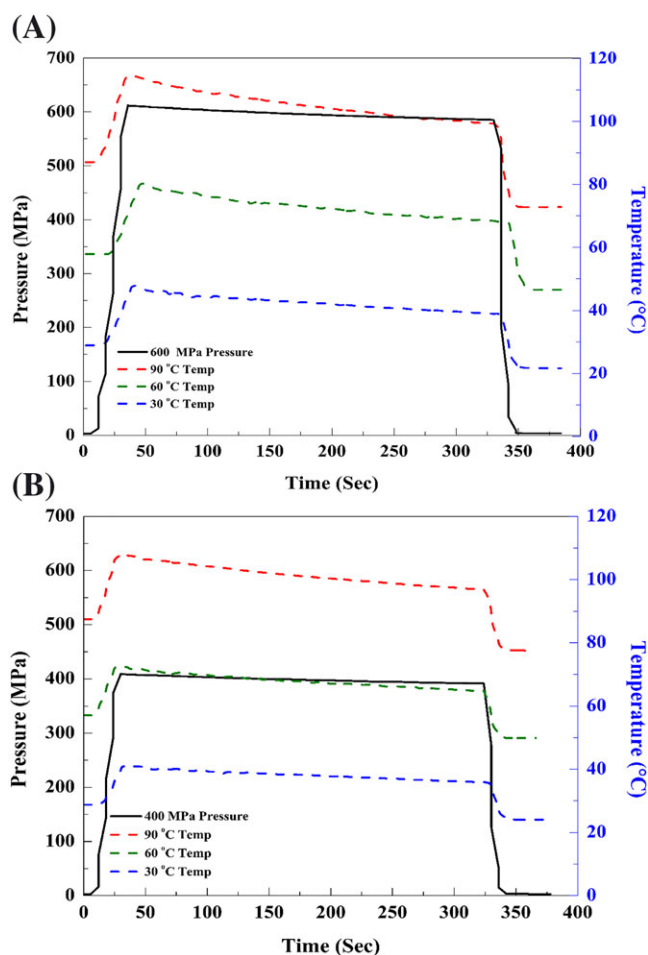
### 3.1 | High-pressure process profiles

Figure 2A and B shows the vessel temperature and pressure changes during the process. Starting initial temperatures were  $90^\circ\text{C}$ ,  $60^\circ\text{C}$ , and  $30^\circ\text{C}$ . The temperatures rapidly increased to  $108^\circ\text{C}$ ,  $70^\circ\text{C}$ , and  $40^\circ\text{C}$  at 400 MPa and to  $115^\circ\text{C}$ ,  $80^\circ\text{C}$ , and  $45^\circ\text{C}$  at 600 MPa, respectively. During the holding period in the HPP vessel, the fluid temperature gradually decreased by  $5^\circ\text{C}$  to  $10^\circ\text{C}$ , depending upon the pressure and initial temperature. The polyoxymethylene insulation sleeve helped to maintain the medium temperature and limited temperature loss to a maximum of  $10^\circ\text{C}$ . Without the insulation, the temperature drop reached up to  $20^\circ\text{C}$  in pretrial. The increase in temperature of the fluid medium within the HPP chamber was due to adiabatic heating within the vessel upon applying the pressure. The increase in temperature was controlled mainly by the initial vessel temperature and the final vessel pressure. The range of pressures and temperatures selected for these experiments represents the conditions of pasteurization and high PATs.<sup>21</sup> A similar increase in temperature at this pressure range and temperature profiles has been previously observed.<sup>22–24</sup>

### 3.2 | Films characterization

#### 3.2.1 | White spots and delamination

Packages that were processed after vacuum packing (approximately 0-cc air/mL  $\text{H}_2\text{O}$  headspace) did not experience any visual physical damage under the processing conditions tested here at up to 600 MPa and



**FIGURE 2** Temperatures and pressure profiles inside the vessel at 600 MPa (A) and 400 MPa (B)

$90^\circ\text{C}$  (Figure 3A and C). Similar results have been reported for other types of packaging held under combined high pressure and temperature.<sup>8,22,25,26</sup> Two forms of physical damage were observed on the processed pouches with 0.30-cc air/mL  $\text{H}_2\text{O}$  headspace and processing temperature above  $30^\circ\text{C}$  (Figure 3B and D). The two forms of defects were white spots in film A EVOH-based and B  $\text{AlO}_x$ -coated PET and delamination only in film B. Results showed that the area of the white spots was significantly ( $P < 0.05$ ) influenced by the package headspace greater than or equal to 0.05-cc air/mL  $\text{H}_2\text{O}$  and starting process temperatures higher than  $30^\circ\text{C}$  (Figure 4). A headspace of 0.25-cc air/mL  $\text{H}_2\text{O}$  resulted in the highest white spot area among all introduced headspace volumes 0.05 to 0.30-cc air/mL  $\text{H}_2\text{O}$ , except for 0.20-cc air/mL  $\text{H}_2\text{O}$ . Delamination took the form of small bubbles localized around the pouch edges. In all cases, defects of either white spots or delamination were located around the edges and the upper part of the pouch near the headspace (Figures 1 and 3).

Pouches processed at  $30^\circ\text{C}$  also did not show defects at any tested headspace or pressure conditions, as previously observed.<sup>14</sup> However, increasing the temperature to  $60^\circ\text{C}$  and  $90^\circ\text{C}$  increased the area of white spots for both films A and B processed at 400 and 600 MPa. Film A showed a white spot area 18% larger compared to film B when processed under the same conditions. This difference may be due to



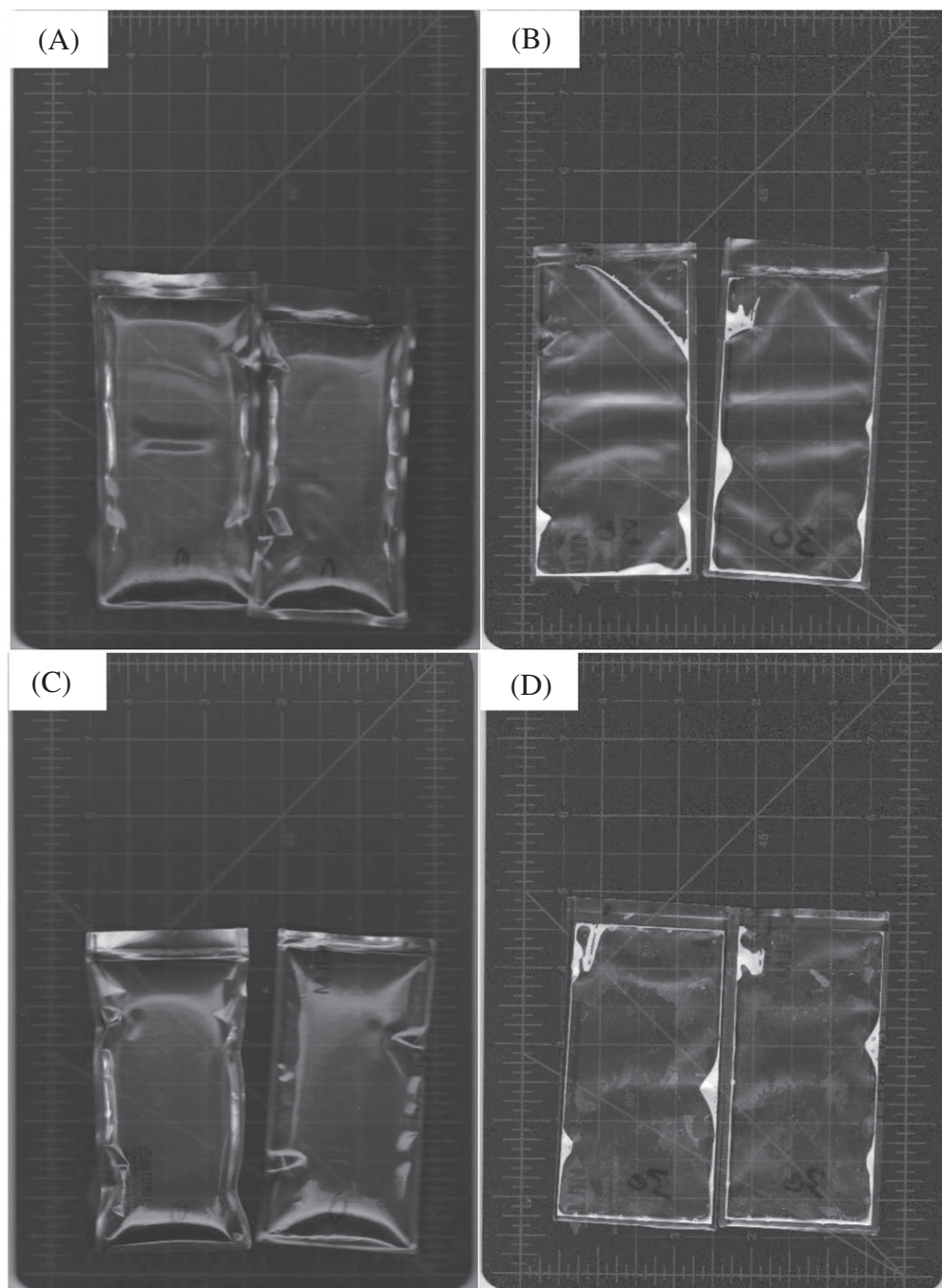


**FIGURE 3** Representative images for film A processed at 400 MPa and 60°C, (A) 0-cc air/mL H<sub>2</sub>O headspace, and (B) 30-cc air/mL H<sub>2</sub>O headspace; film B processed at 400 MPa and 60°C, (C) 0-cc air/mL H<sub>2</sub>O headspace, and (D) 30-cc air/mL H<sub>2</sub>O headspace

bubble formation in film B. In addition, the level of this defect was slightly higher in film A at a higher pressure of 600 MPa. However, the level of defect was only marginally higher in film B for the process at lower pressure of 400 MPa. This increase may be due to a higher bubble formation at 600 MPa in the white spot area. Despite the small variation, overall pressure levels did not show significant differences in the damage for both films.

When a high-pressure process is combined with an elevated temperature above 30°C, the package headspace becomes a more critical factor that should be considered in the process design. A headspace as

small as 0.05-cc air/mL H<sub>2</sub>O could result in noticeable damage. Hence, for the PATS process, residual gas in the packaging should be minimized. Some food products may contain entrained residual air that is released upon the application of pressure.<sup>27</sup> However, high-pressure pasteurization at low temperatures less than or equal to 30°C can allow for residual gases.<sup>28</sup>

Delamination only occurred when the metal element was present in the packaging as a coated barrier layer.<sup>14,29,30</sup> Another major difference between films A and B is that film A with the EVOH-base was coextruded while PET-coated AlO<sub>x</sub> film B was laminated. The

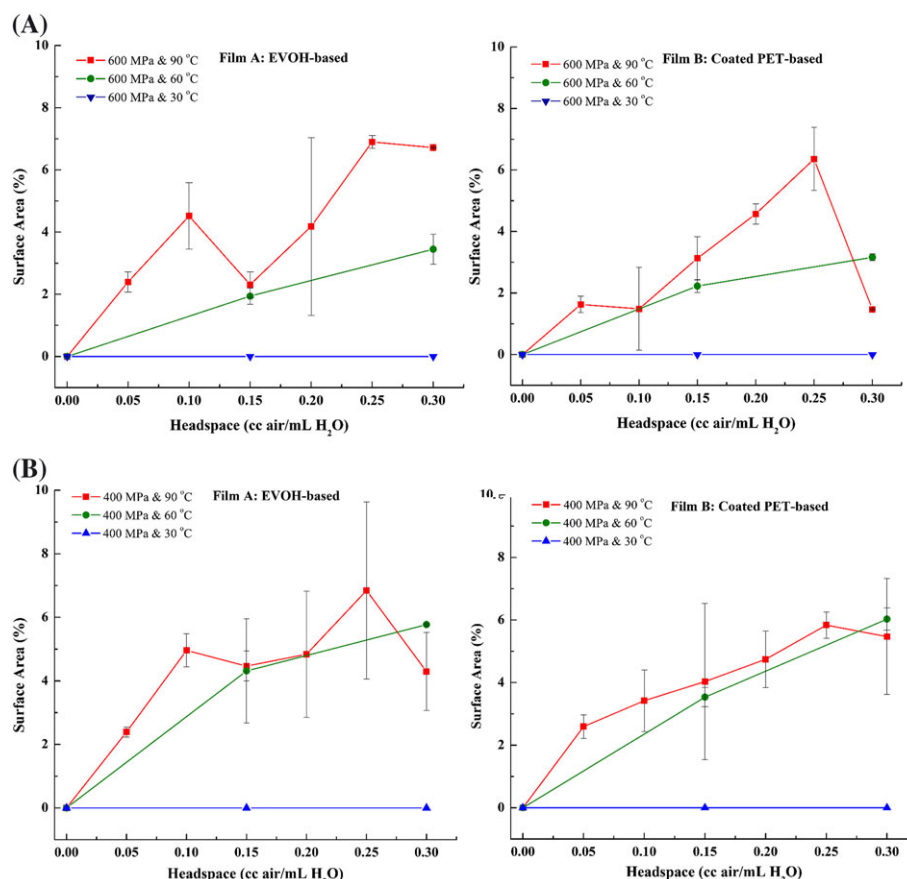


**FIGURE 4** Influence of headspace air volume on the defected area as a percentage; (A) at 600 MPa and (B) at 400 MPa ( $n = 3$ )

molecular bonding in coextruded film structure is generally stronger than laminated structures. Although films A and B were made of different polymers, the cohesive force that bound and held the layers together may be lower in film B than in film A, making delamination more apparent in film B. Sterr et al in 2017 proposed that fast decompression causes a blistering effect from explosive decompression failure.<sup>31</sup> In addition to analysing the white spots and delamination, the physical, thermal, mechanical, and structural properties of the film structures were examined.

### 3.2.2 | Colour and thickness

To demonstrate the effect of different processes on the package using a relatively simple test, the overall colour change ( $\Delta E$ ) and lightness ( $L^*$ ) of white spots and (visually) unaffected area (where white spots were not present) of both films were measured. This was performed at the most extreme process conditions tested in this study, 90°C, 600 MPa, and 0.30-cc air/mL  $H_2O$  headspace. The  $\Delta E$  of white spots on film A was higher than those on film B (Figure 5) because no delamination occurred in film A. Thus, stress was concentrated on the film layers PP, EVOH, and PA. However, in film B, the inner layer (PP) was delaminated and formed small bubbles. The physical stress of the high-pressure and high-temperature process created more white spots on film A. The damaged area (white spots) in film B was lower because the film may have exhibited failure stress, resulting in delamination.

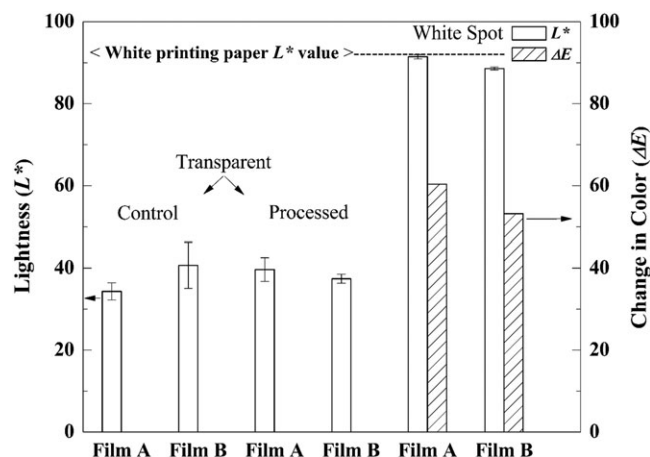


**FIGURE 5** White spots' lightness value relative to the transparent package and white printing paper ( $n = 3$ )

The  $L^*$  values of white spots on films were close to the lightness value of white printing paper. This whiteness (stress whiteness) was primarily caused by small voids, surface cracks, wrinkles, as well as macro-size chain reorientation and stretching from stress applied to the polymers.<sup>32-34</sup> Overall, the formation of white spots is undesirable.<sup>35</sup> The  $L^*$  of the unaffected area of film A was lower compared with the same of film B, but the values did not differ significantly ( $P > 0.05$ ) from the values of unprocessed films.

**TABLE 1** Overall thickness of the control and processed films and white spots ( $n = 3$ )

Film	Thickness, $\mu\text{m}$		White Spot
	Control	Processed	
A	$92.3 \pm 0.6^{\text{aA}}$	$92.7 \pm 0.6^{\text{aA}}$	$130.7 \pm 19.9^{\text{bA}}$
B*	$79.3 \pm 1.2^{\text{aB}}$	$82.0 \pm 1.7^{\text{aB}}$	$164.3 \pm 19.6^{\text{bA}}$

The same small superscript letters in the same row and capital letters in the same column do not differ significantly at  $\alpha = 0.05$ .

\*Bubbles ranging diameter up to 5 mm were also observed in the film B.

The thickness of white spots in film B was slightly higher but not statistically different ( $P > 0.05$ ) than the white spot thickness in film A (Table 1). The overall thicknesses of the remaining areas of the films were not affected after processing. The significant increase in film thickness at the white spots confirmed the changes in the topography and morphology of the films, as stated previously. The changes included cracks, voids, and wrinkles were also reported elsewhere.<sup>36</sup> In addition, bubbles with a diameter of up to 5 mm formed in film B. Other researchers have also reported bubble formation in PET-based multi-layer films after high-pressure and high-temperature processing.<sup>9,37</sup>

### 3.2.3 | Thermal analysis

Both films A and B generally showed good thermal stability in terms of the melting temperature ( $T_m$ ) of individual layers and total enthalpy ( $\Delta H$ ). For film A, the  $T_m$  of individual layers and  $\Delta H$  were not affected after processing (Table 2). For film B, the  $T_m$  of different layers was not affected by the high-pressure and high-temperature processing, while  $\Delta H$  increased from  $32.3 \pm 2.4$  to  $38.1 \pm 1.4$  J/g after processing at 90°C and 600 MPa. The increase in enthalpy may be attributed to chain reorientation and alignment at high-processing temperatures.<sup>38</sup> An increase of melting enthalpy was previously reported for PET and 27% mol ethylene EVOH-based films.<sup>8,39</sup> The  $T_m$  and  $\Delta H$  of white spots did not differ significantly ( $P > 0.05$ ) from the same of the undamaged regions of processed films. López-Rubio et al in 2005 studied the effect of high-pressure and high-temperature treatment on two EVOH films of 26 and 48 mol% of ethylene content.<sup>25</sup> They found that the ethylene content in EVOH films influenced the level

of impact on barrier and thermal properties of films subjected to high-pressure and high-temperature process.

### 3.2.4 | Mechanical properties

The tensile strength, elongation at the break, and sealing strength of film A did not change after processing. However, the mechanical properties of film B decreased significantly ( $P < 0.05$ ) after processing at 90°C and 600 MPa, except for elongation at break (Table 3). The limited sealing strength for film B could be because of the bubble formation around the sealed edges, with a decreased strength by around 20%. Pinholes and cracks induced by the thermal stress may have decreased the tensile strength by 15%.<sup>20</sup> Galotto et al in 2008 made a similar observation for PET coated with metal oxide and PP-based pouches containing aqueous simulant and olive oil subjected to 60°C and 400 MPa processing. They also observed cracks and pinholes in the studied films.<sup>11</sup>

### 3.2.5 | Barrier properties

Figure 6A and B shows the effect of high pressure and temperature on OTR and WVTR for films A and B. The OTR of films A and B did not change after processing at 30°C and 600 MPa. However, the OTR of film B increased significantly ( $P < 0.05$ ) when the process temperature increased to 90°C. The oxygen barrier change in film B was much higher, increasing the OTR from 0.02 to 12.4  $\text{cm}^3/\text{m}^2/\text{day}$ . For film A, the OTR increased from 1.2 to 2.2  $\text{cm}^3/\text{m}^2/\text{day}$  (Figure 6A). The WVTR of film A was not affected by low (30°C) or high (90°C) temperature and pressure (600 MPa) processes at 6.7 to 6.6  $\text{g}/\text{m}^2/\text{day}$  (Figure 6B). In contrast, the WVTR of film B increased significantly ( $P < 0.05$ ) from 0.4 to 5  $\text{g}/\text{m}^2/\text{day}$  when processed at 90°C and 600 MPa. Zhang et al<sup>40</sup> made similar observations for the barrier properties of PP/EVOH/PA film subjected to microwave-assisted thermal sterilization. In that study, the OTR doubled while the WVTR remained the same compared with unprocessed films, despite the difference in processing.<sup>41</sup> In our study, film B showed poor performance when subjected to 90°C and 600-MPa processing. The deterioration of the barrier properties for film B was in line with the degradation in its mechanical properties. These changes can be attributed to the cracks and pinholes may have developed in film B. The properties of gas barrier are critical to the shelf life of packaged

**TABLE 2** Thermal properties of the individual layers in film structures A and B ( $n = 3$ )

Film	Layer	Control		Processed*		White Spot	
		$T_m$ , °C	$\Delta H^{**}$ , J/g	$T_m$ , °C	$\Delta H$ , J/g	$T_m$ , °C	$\Delta H$ , J/g
A	PP	$164.4 \pm 0.2^{\text{a}}$	$33.4 \pm 4.5^{\text{A}}$	$165.0 \pm 0.1^{\text{a}}$	$29.1 \pm 4.0^{\text{A}}$	$164.7 \pm 0.2^{\text{a}}$	$31.5 \pm 5.3^{\text{A}}$
	EVOH	$180.7 \pm 4.2^{\text{a}}$		$182.0 \pm 4.8^{\text{a}}$		$182.2 \pm 1.8^{\text{a}}$	
	PA	$223.2 \pm 1.4^{\text{a}}$		$223.2 \pm 2.6^{\text{a}}$		$223.0 \pm 0.9^{\text{a}}$	
B	OC	$126.5 \pm 0.1^{\text{a}}$	$32.3 \pm 2.4^{\text{A}}$	$126.7 \pm 0.0^{\text{a}}$	$38.1 \pm 1.4^{\text{B}}$	$126.6 \pm 0.1^{\text{a}}$	$38.4 \pm 0.1^{\text{B}}$
	PP	$166.2 \pm 0.1^{\text{a}}$		$166.3 \pm 0.2^{\text{a}}$		$165.9 \pm 0.2^{\text{a}}$	
	PA	$223.7 \pm 0.6^{\text{a}}$		$224.2 \pm 0.3^{\text{a}}$		$223.4 \pm 1.1^{\text{a}}$	
	PET	$257.8 \pm 0.1^{\text{a}}$		$258.0 \pm 0.2^{\text{a}}$		$258.1 \pm 0.1^{\text{a}}$	

Same small or capital superscript letters in the same row do not differ significantly at  $\alpha = 0.05$ .

\*Processed at 600 MPa and 90°C.

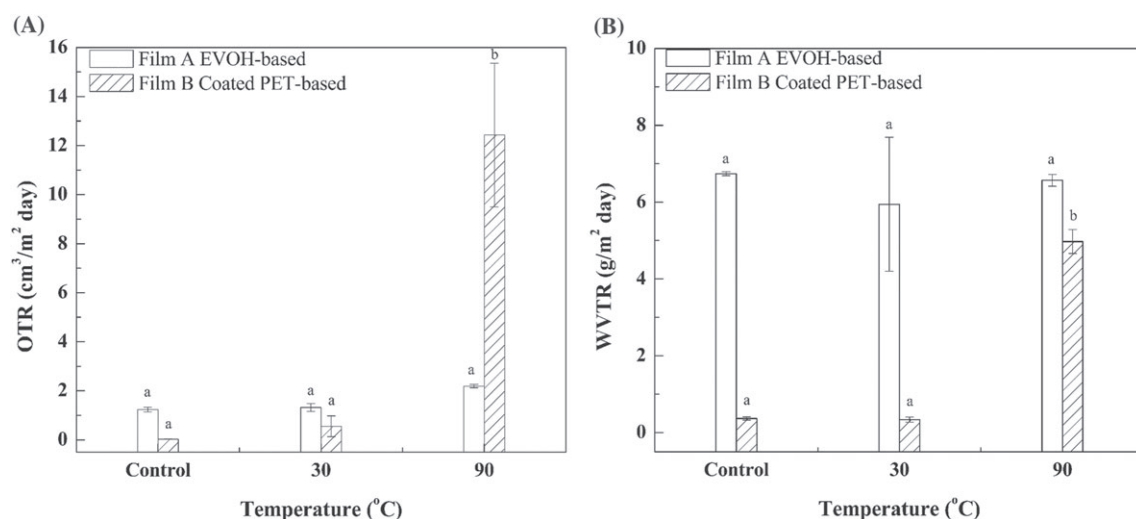
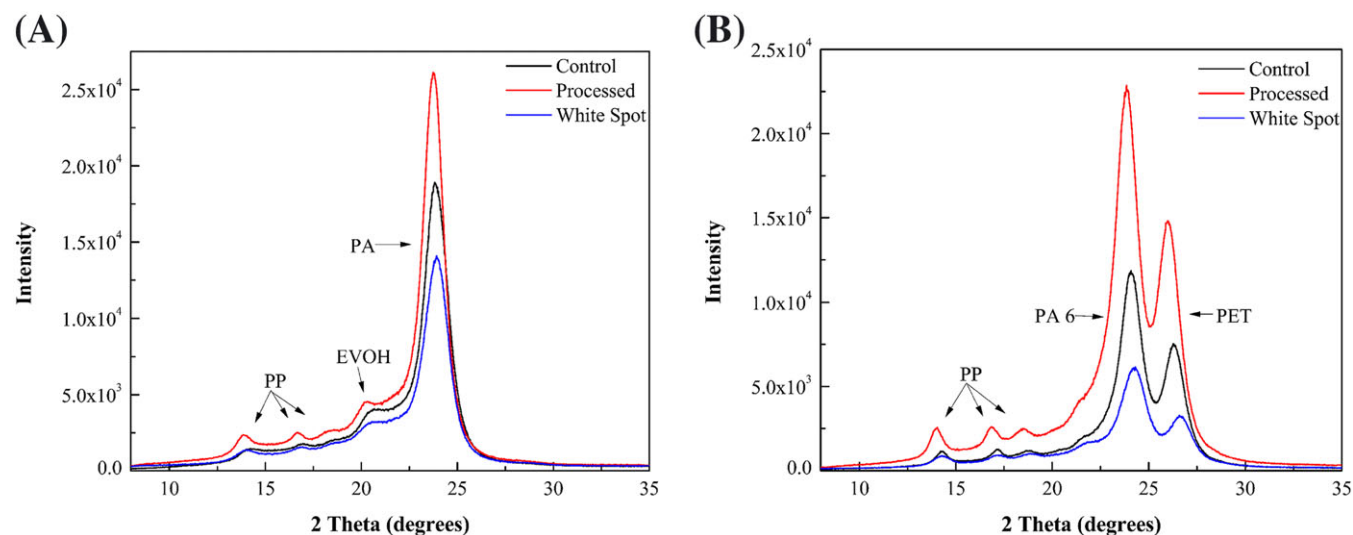
\*\*Total melting enthalpy ( $\Delta H = \Delta H_{\text{PP}} + \Delta H_{\text{EVOH}} + \Delta H_{\text{PA}}$ ).

**TABLE 3** Mechanical properties of films A and B at 25 ± 2°C (n = 5)

Process		Film A			Film B		
Pressure, MPa	Temperature, °C	Tensile strength, MPa	Elongation at break, %	Sealing strength*, MPa	Tensile strength, MPa	Elongation at break, %	Sealing strength*, MPa
Control	25	54.4 ± 6.0 <sup>a</sup>	96.9 ± 20.5 <sup>a</sup>	34.0 ± 2.0 <sup>a</sup>	70.9 ± 4.5 <sup>a</sup>	67.9 ± 4.1 <sup>a</sup>	44.7 ± 2.7 <sup>a</sup>
600	90	54.7 ± 4.6 <sup>a</sup>	93.8 ± 42.0 <sup>a</sup>	31.1 ± 4.1 <sup>a</sup>	59.9 ± 4.0 <sup>b</sup>	62.1 ± 8.2 <sup>a</sup>	35.8 ± 6.2 <sup>b</sup>

Same small superscript letters in the same column do not differ significantly at  $\alpha = 0.05$ . Across sectional area = thickness of the film × width of the tested strip.

\*Film samples tested included the white spots on the film edges.

**FIGURE 6** Oxygen (A) and water vapour (B) transmission rate of processed packages at 600 MPa (n = 3)**FIGURE 7** X-ray diffraction intensity of film (A) A and (B) B control, processed, and white spots on the films processed at 600 MPa and 90°C

foods.<sup>40</sup> Mild temperatures combined with high pressure do not tend to change the barrier properties of multilayer films, and temperature appears to be the predominant effect that leads to loss in barrier properties.<sup>14</sup>

### 3.2.6 | X-ray diffraction

The X-ray diffractograms for control, processed films, and white spot areas for films A and B, processed at 600 MPa and 90°C, are



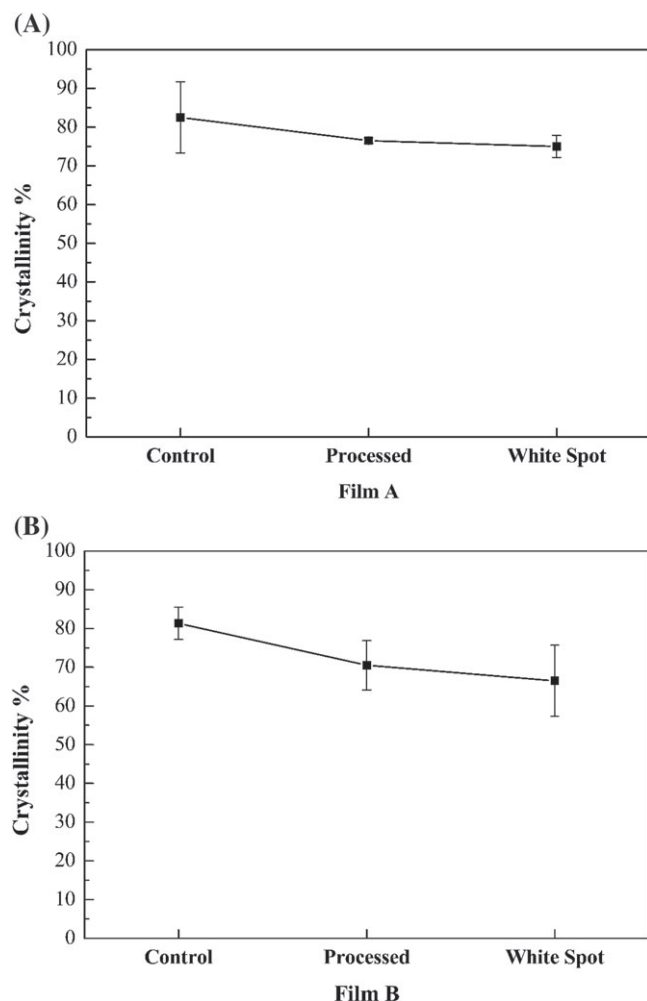


**FIGURE 8** Overall crystallinity percentage of EVOH-based (A) film A and (B) coated PET-based film B; control, processed, and white spots on the films processed at 600 MPa and 90°C (n = 3)

presented in Figure 7A and B. The peaks were identified by the ICDD database and compared with the literature.<sup>20</sup> film A exhibited three peaks for the PP layer at  $2\theta$  equalling 13° and 14°, 16° and 17°, and 18° and 19°. These peaks were also observed for the PP layer in film B. The EVOH layer in film A exhibited a peak around the 20° band. The PA peak was most prominent and appeared at 23° to 24°. In film B, the PA peak appeared at 24° and the PET peak appeared at 26°.

The crystallinity percentages of films A and B are plotted in Figure 8A and B. The overall crystallinity of the EVOH-based film A decreased slightly from 82% to 76% after processing at 600 MPa and 90°C. The white spot area showed a 1.5% further decrease to 75%. However, the decrease in crystallinity was not statistically significant ( $P > 0.05$ ). The initial reduction in crystallinity of the EVOH-based film could be due to plasticization by water (food simulant) absorbed during the process.<sup>38,42,43</sup> The insignificant decrease in crystallinity of film A in the white spot may be due to the change in topography rather than the change in the morphology of the film's inner layer. In contrast, film B showed a decrease in crystallinity of about 11% after processing at

600 MPa and 90°C, decreasing from 81% to 70%. However, the white spot area in film B showed a further decrease in crystallinity to 66%. A relatively small reduction in crystallinity and chain reorientation, especially in film B, resulted in changes to the barrier, thermal, and mechanical properties, as discussed previously. Sterr et al reported similar trends in crystallinity changes in PET film coated with metal oxide. They found that the in the amorphous region in the PET  $\text{SiO}_x$ -based lid film increased as the package headspace increased from 15% to 50%.<sup>17</sup> This reduction in the crystalline region may be attributed to the shear force applied between layers as they attempted to rearrange and delaminate. This reduction accorded with our visual observations, in which the loss of transparency and whitening occurred in both films A and B.

## 4 | CONCLUSIONS

Headspace resulted in physical damage to the package in the form of whitening stress (white spots) and/or delamination in high-pressure and high-temperature processes. However, visual defects were not observed at lower temperatures (30°C) and pressures between 400 and 600 MPa at package headspace of values up to 0.30-cc air/mL  $\text{H}_2\text{O}$ . The primary visual change in coextruded film A (PA/EVOH/PP) was the white spot, which did not alter the mechanical and thermal properties of EVOH-based film A. The delamination in the form of small bubbles also occurred in PET film B coated with metal oxide (PET- $\text{AlO}_x$ -OC/PA 6/PP) and affected its mechanical, thermal, and barrier properties. Overall, the performance of EVOH-based film was better than that of the coated PET-based film in the thermal, mechanical, and barrier properties. Therefore, physical damage to multilayer film packaging during high-pressure and high-temperature processing can be minimized by reducing the headspace. The findings may inform food manufacturers in the selection of polymer packaging and package headspace for high-pressure and high-temperature processes.

## ACKNOWLEDGEMENTS

The authors would like to acknowledge the financial support of USDA National Institute of Food and Agriculture (NIFA) research grants # 2016-67017-24597 and the Washington State University Agriculture Experiment Station. Saleh Al-Ghamdi also would like to thank King Saud University for his PhD scholarship.

## ORCID

Saleh Al-Ghamdi <https://orcid.org/0000-0001-5230-5314>

Shyam S. Sablani <https://orcid.org/0000-0001-5602-3832>

## REFERENCES

- Balasubramaniam V, Barbosa-Cánovas GV, Lelieveld HL. *High Pressure Processing of Food*. New York: Springer-Verlag; 2016.
- Huang HW, Wu SJ, Lu JK, Shyu YT, Wang CY. Current status and future trends of high-pressure processing in food industry. *Food Control*. 2017;72:1-8.
- Hendrickx M, Ludikhuyze L, Van den Broeck I, Weemaes C. Effects of high pressure on enzymes related to food quality. *Trends Food Sci Technol*. 1998;9(5):197-203.

4. Sun N, Lee S, Song KB. Effect of high-pressure treatment on the molecular properties of mushroom polyphenoloxidase. *LWT-Food Sci Technol*. 2002;35(4):315-318.
5. Palou E, Hernández-Salgado C, López-Malo A, Barbosa-Cánovas G, Swanson B, Welti-Chanes J. High pressure-processed guacamole. *Innov Food Sci Emerg Technol*. 2000;1(1):69-75.
6. Richter T, Sterr J, Jost V, Langowski H-C. High pressure-induced structural effects in plastic packaging. *High Pressure Res*. 2010;30(4):555-566.
7. Fradin J, Le Bail A, Sanz P, Molina-Garcia A. Note. Behaviour of packaging materials during high pressure thawing nota. Comportamiento del material para el envase durante la descongelación con altas presiones. *Revista de Agaroquímica Y Tecnología de Alimentos*. 1998;4(6):419-424.
8. Dhawan S, Barbosa-Cánovas GV, Tang J, Sablani SS. Oxygen barrier and enthalpy of melting of multilayer EVOH films after pressure-assisted thermal processing and during storage. *J Appl Polym Sci*. 2011;122(3):1538-1545.
9. Mensitieri G, Fraldi M. Flexible packaging for high pressure treatments: delamination onset and design criteria of multilayer structures. *J Appl Packag Res*. 2016;8(4):2.
10. Schauwecker A, Balasubramaniam V, Sadler G, Pascall M, Adhikari C. Influence of high-pressure processing on selected polymeric materials and on the migration of a pressure-transmitting fluid. *Packag Technol Sci*. 2002;15(5):255-262.
11. Galotto MJ, Ulloa P, Hernández D, Fernández-Martín F, Gavara R, Guarda A. Mechanical and thermal behaviour of flexible food packaging polymeric films materials under high pressure/temperature treatments. *Packag Technol Sci*. 2008;21(5):297-308.
12. Bull M, Steele R, Kelly M, Olivier S, Chapman B. Packaging under pressure: effects of high pressure, high temperature processing on the barrier properties of commonly available packaging materials. *Innov Food Sci Emerg Technol*. 2010;11(4):533-537.
13. Filimon V, Borda D, Alexe P, Stoica M. Study of PATP impact on food packaging materials. *Materiale Plastice*. 2016;53(1):48-51.
14. Juliano P, Koutchma T, Sui Q, Barbosa-Cánovas GV, Sadler G. Polymeric-based food packaging for high-pressure processing. *Food Eng Rev*. 2010;2(4):274-297.
15. Richter, T., Multivac Sepp Hagenmueller GmbH and Co KG, assignee. Device and method for the high-pressure treatment of products. U.S. Patent 8,771,773.2014.
16. Caner C, Hernandez RJ, Pascall MA, Reimer J. The use of mechanical analyses, scanning electron microscopy and ultrasonic imaging to study the effects of high-pressure processing on multilayer films. *J Sci Food Agr*. 2003;83(11):1095-1103.
17. Sterr J, Fleckenstein BS, Langowski HC. The effect of high-pressure processing on tray packages with modified atmosphere. *Food Eng Rev*. 2015;7(2):209-221.
18. Fairclough J, Conti M. Influence of ultra-high pressure sterilization on the structure of polymer films. *Packag Technol Sci*. 2009;22(5):303-310.
19. Al-Ghamdi S. *Synthesis of nanoporous carbohydrate metal-organic framework and encapsulation of selected organic compounds*. Michigan State University: ProQuest LLC; 2014.
20. Zhang H, Bhunia K, Munoz N, et al. Linking morphology changes to barrier properties of polymeric packaging for microwave-assisted thermal sterilized food. *J Appl Polym Sci*. 2017;134(44).
21. Mújica-Paz H, Valdez-Fragoso A, Samson CT, Welti-Chanes J, Torres JA. High-pressure processing technologies for the pasteurization and sterilization of foods. *Food Bioproc Tech*. 2011;4(6):969-985.
22. Dhawan S, Varney C, Barbosa-Canovas GV, Tang J, Selim F, Sablani SS. Pressure-assisted thermal sterilization effects on gas barrier, morphological, and free volume properties of multilayer EVOH films. *J Food Eng*. 2014;128:40-45.
23. Barbosa-Cánovas GV, Juliano P. Food sterilization by combining high pressure and thermal energy. In: *Food Engineering: Integrated Approaches*. New York, NY: Springer; 2008:9-46.
24. Rasanayagam V, Balasubramaniam V, Ting E, Sizer C, Bush C, Anderson C. Compression heating of selected fatty food materials during high-pressure processing. *J Food Sci*. 2003;68(1):254-259.
25. López-Rubio A, Lagarón JM, Hernández-Muñoz P, et al. Effect of high pressure treatments on the properties of EVOH-based food packaging materials. *Innov Food Sci Emerg Technol*. 2005;6(1):51-58.
26. Halim L, Pascall M, Lee J, Finnigan B. Effect of pasteurization, high-pressure processing, and retorting on the barrier properties of nylon 6, nylon 6/ethylene vinyl alcohol, and nylon 6/nanocomposites films. *J Food Sci*. 2009;74(1):N9-N15.
27. Yan H, Barbosa-Cánovas G. Density changes in selected agglomerated food powders due to high hydrostatic pressure. *LWT-Food Sci Technol*. 2001;34(8):495-501.
28. Amanatidou A, Schlüter O, Lemkau K, Gorris L, Smid E, Knorr D. Effect of combined application of high pressure treatment and modified atmospheres on the shelf life of fresh Atlantic salmon. *Innov Food Sci Emerg Technol*. 2000;1(2):87-98.
29. Caner C, Hernandez RJ, Harte BR. High-pressure processing effects on the mechanical, barrier and mass transfer properties of food packaging flexible structures: a critical review. *Packag Technol Sci*. 2004;17(1):23-29.
30. Sansone L, Aldi A, Musto P, Amendola E, Mensitieri G. Effects of high pressure treatments on polymeric films for flexible food packaging. *Packag Technol Sci*. 2014;27(9):739-761.
31. Sterr J, Fleckenstein BS, Langowski H-C. The theory of decompression failure in polymers during the high-pressure processing of food. *Food Eng Rev*. 2018;10(1):14-33. <https://doi.org/10.1007/s12393-017-9171-9>
32. Bucknall C, Smith R. Stress-whitening in high-impact polystyrenes. *Polymer*. 1965;6(8):437-446.
33. Hadal R, Yuan Q, Jog J, Misra R. On stress whitening during surface deformation in clay-containing polymer nanocomposites: a microstructural approach. *Mater Sci Eng A*. 2006;418(1):268-281.
34. Liu Y, Kennard CH, Truss RW, Calos NJ. Characterization of stress-whitening of tensile yielded isotactic polypropylene. *Polymer*. 1997;38(11):2797-2805.
35. Kohan-nia N, Pakbin B, Mahmoudi R, Fakhri O. Effect of packaging material on color properties of catsup tomato sauce. *J Appl Packag Res*. 2016;8(2):4.
36. Fleckenstein BS, Sterr J, Langowski HC. The effect of high pressure processing on the integrity of polymeric packaging-analysis and categorization of occurring defects. *Packag Technol Sci*. 2014;27(2):83-103.
37. Zhao W, Liu D, Zhang Y. Study on the Influence of Pressure-Assisted Thermal Processing on PET/PE via the Change of Melting Enthalpy. *J Food Process Preserv*. 2017;41:e13135. <https://doi.org/10.1111/jfpp.13135>
38. Selke SE, Culter JD. *Plastics Packaging: Properties, Processing, Applications, and Regulations*. 3rd ed. Munich, Germany: Hanser; 2016.
39. Bhunia K, Zhang H, Liu F, Rasco B, Tang J, Sablani SS. Morphological changes in multilayer polymeric films induced after microwave-assisted pasteurization. *Innov Food Sci Emerg Technol*. 2016;38:124-130.
40. Zhang HC, Tang ZW, Rasco B, Tang JM, Sablani SS. Shelf-life modeling of microwave-assisted thermal sterilized mashed potato in polymeric pouches of different gas barrier properties. *J Food Eng*. 2016;183:65-73.

41. Zhang HC, Bhunia K, Kuang PQ, et al. Effects of oxygen and water vapor transmission rates of polymeric pouches on oxidative changes of microwave-sterilized mashed potato. *Food Bioproc Tech*. 2016;9(2):341-351.
42. Cerruti P, Laurienzo P, Malinconico M, Carfagna C. Thermal oxidative stability and effect of water on gas transport and mechanical properties in PA6-EVOH films. *J Polym Sci B*. 2007;45(7):840-849.
43. Robertson GL. *Food Packaging: Principles and Practice*. Boca Raton, FL: CRC press; 2013.

**How to cite this article:** Al-Ghamdi S, Rasco B, Tang J, Barbosa-Cánovas GV, Sablani SS. Role of package headspace on multilayer films subjected to high hydrostatic pressure. *Packag Technol Sci*. 2019;32:247-257. <https://doi.org/10.1002/pts.2432>